

On the Secrecy Performance Over N-Wave with Diffuse Power Fading Channel

José David Vega Sánchez, D. P. Moya Osorio, F. Javier López-Martínez, Martha Cecilia Paredes, and Luis Urquiza-Aguiar

arXiv:2002.05206v2 [eess.SP] 15 Mar 2020

Abstract—We investigate the effect of considering realistic propagation conditions different from classical Rice and Rayleigh fading on wireless physical layer security. Specifically, we study how the superposition of a number of dominant specular waves and diffusely propagating components impacts the achievable secrecy performance compared to conventional assumptions relying on the central limit theorem. We derive analytical expressions for the secrecy outage probability, which have similar complexity to other alternatives in the literature derived for simpler fading models. We provide very useful insights on the impact on physical layer security of (i) the number; (ii) the relative amplitudes and (iii) the overall power of the dominant specular components. We show that it is possible to obtain remarkable improvements on the system secrecy performance when: (a) the relative amplitudes of the dominant specular components for the eavesdropper channel are sufficiently large compared to those of the eavesdropper's channel eavesdropper, and (b) the power of Bob's dominant components is significantly larger than the power of the Eve's dominant components.

Index Terms—generalized fading channels, mm-Wave, N-wave with diffuse power fading model, physical layer security.

I. INTRODUCTION

THE fifth-generation (5G) of mobile networks aims to raise the capacity and performance of communication systems to unprecedented levels, including ultra-high data rates, ultra-wide radio coverage, massive simultaneously connected devices and ultra-low latencies. The new scenarios of wireless systems under the umbrella of 5G include mm-Wave, device-to-device, machine-type, and vehicular communications, among many others [1]. In particular, recent investigations have shown that none of the well-established fading models (e.g., Rayleigh, Rician and Nakagami- m) present accurate fit with field measurements in mm-Wave communications [2]. One of the reasons for such mismatch relies in the fact that classical fading models heavily rely on the central limit theorem (CLT), which assumes a sufficiently large number of multipath waves arriving at the receiver ends – and such conditions are not always met [3].

In the last years, some efforts have been oriented to formulate more accurate channel models that overcome such limi-

tation. Among them, stochastic fading models that explicitly discern between the individual multipath waves classically regarded as line-of-sight (LOS) components have been proposed as a way for bridging the gap between CLT-based approaches and purely ray-based models. Durgin's two-wave with diffuse power (TWDP) [4] and its generalization in [5] are known to improve the fit to field measurements in different scenarios including mm-Wave set-ups [2, 6], compared to conventional small-scale fading models.

On the other hand, a myriad of challenges must still be overcome so that 5G converges into a reliable, safe and efficient system. One of the most critical aspects is related to the security of information transmission, given that 5G is designed to support rather diverse applications. As a consequence, highly confidential and vulnerable data is expected to be transmitted in future 5G and beyond networks, which because of their wireless nature are sensitive to eavesdropping. Regarding this, physical layer security (PLS) [7] emerges as a promising solution to complement traditional security systems by taking advantage of the random nature of wireless channels to provide lightweight and efficient solutions for increasing the security level in some applications [8, 9].

The physical layer security performance in wireless channels is a rather well-investigated topic in the literature. Nevertheless, because of the intricate nature of physically-motivated wireless fading models, available results are restricted to some special cases [10, 11] on which only two specular components are considered. Very recently, it was suggested in [12] that the inability to achieve perfect secrecy in wireless channels was an artifact due to the consideration of the CLT assumption. Hence, the impact of the number of multipath waves arriving at the receiver ends, as well as their relative amplitudes, has a dramatical effect on the secrecy performance. However, the results in [12] considered only the limit case of a total absence of diffuse fading, and the derivation of analytical expressions for the secrecy performance metrics was not possible for an arbitrary number of waves.

In this paper, we investigate the PLS performance in a wireless set-up, by assuming that the received signal is built from the superposition of an arbitrary number N of dominant multipath waves, plus some additional diffuse components – this will be referred to as N-wave with diffuse power (NWDP) fading, for which some formulations have been recently proposed in order to deal with its rather unwieldy nature [13, 14]. Our goal is to perform a fine-grain characterization of the role of individual multipath waves on the secrecy performance, and to support our findings with analytical results. We derive

José David Vega Sánchez, Martha Cecilia Paredes, and Luis Urquiza-Aguiar are with the Departamento de Electrónica, Telecomunicaciones y Redes de Información, Escuela Politécnica Nacional (EPN), Quito, 170525, Ecuador. (e-mail: jose.vega01@epn.edu.ec; cecilia.paredes@epn.edu.ec; luis.urquiza@epn.edu.ec)

D. P. Moya Osorio is with the Centre for Wireless Communications (CWC), University of Oulu, Finland. (e-mail: diana.moyaosorio@oulu.fi)

F. Javier López-Martínez is with Departamento de Ingeniería de Comunicaciones, Universidad de Málaga - Campus de Excelencia Internacional Andalucía Tech., Málaga 29071, Spain. (e-mail: fjlopezm@ic.uma.es)

exact expressions for the secrecy outage probability (SOP) for an arbitrary number of dominant waves at the desired and eavesdropping ends, as well as simplified approximations that become asymptotically tight in the high signal-to-noise ratio (SNR) regime. Some useful insights for improving the secrecy performance in this scenario will be derived, which are inherently linked to the underlying propagation mechanisms and characteristics captured by the NWDP fading model. The main contributions of this paper are as follows:

- An exact closed-form expression for the SOP in terms of well-know functions for the classical Wyner's channel model under NWDP fading.
- A high SNR approximation of the SOP is also derived, which can be used straightforwardly in the context of PLS. The merits of such expression are: (i) when $\bar{\gamma}_E$ is at high SNR regime, it is highly tight to the exact SOP; (ii) it notably reduces the computational effort concerning the exact SOP. This fact helps to the wireless system designers when requiring quick evaluation of security risks.
- Some useful insights into the system are also provided through the asymptotic analysis based on the exact analytical expression of the SOP.

The remainder of this paper is organized as follows. System and channel models are described in Section II. Section III derives closed-form expressions for (i) the SOP; (ii) a high SNR regime of the SOP; (iii) the asymptotic behaviour of the SOP over NWDP fading channel. Section IV shows illustrative numerical results and discussions. Finally, concluding remarks are provided in Section V.

Notation: Throughout this paper, $f_{(Z)}(z)$ and $F_{(Z)}(z)$ denote the probability density function (PDF) and the cumulative distribution function (CDF) of a random variable Z . $\mathbb{E}[\cdot]$ denotes expectation, $\Pr\{\cdot\}$ denotes probability, and $|\cdot|$ denotes the absolute value. In addition, $L_n(\cdot)$ denotes the Laguerre polynomial [15, Eq. (22.2.13)], $\Gamma(\cdot)$ denotes the gamma function [15, Eq. (6.1.1)]; $\gamma(\cdot, \cdot)$, the lower incomplete gamma function [15, Eq. (6.5.2)]; ${}_2F_1(\cdot, \cdot; \cdot; \cdot)$, denotes the hypergeometric function [15, Eq. (15.1.1)], and $(\cdot)_{(\cdot)}$ is the Pochhammer symbol [15, Eq. (6.1.222)].

II. SYSTEM MODEL

We consider the classic Wyner's wiretap channel as depicted in Fig. 1, where a legitimate transmitter Alice (A) sends confidential messages to the legitimate receiver Bob (B) through the main channel, while the eavesdropper Eve (E) tries to intercept these messages from its received signal over the eavesdropper channel. It is assumed that the main and eavesdropper channels experience independent quasi-static fading. Without loss of generality, we assume that all nodes are equipped with a single antenna.

We express the signal at each of the receiving ends as a superposition of N multipath waves arising from dominant specular reflections, and M additional waves associated to diffuse scattering:

$$\mathbf{R} \exp(j\theta) = \sum_{i=1}^N V_i \exp(j\theta_i) + \sum_{k=1}^M V_k \exp(j\theta_k) \quad (1)$$

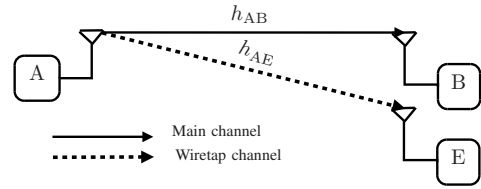


Fig. 1. Wiretap channel consisting of a legitimate pair and one eavesdropper.

Because each diffuse scatterer is able to generate several multipath waves [16], we can safely assume that $M \rightarrow \infty$ and hence the diffuse component¹ tends to be Gaussian distributed, i.e., $\sum_{k=1}^M V_k \exp(j\theta_k) \approx V_d \exp(j\theta_d)$, so that V_d is Rayleigh distributed with $\mathbb{E}\{|V_d|^2\} = 2\sigma^2 = \Omega$.

In (1), $V_i \exp(j\theta_i)$ denotes the i -th specular component having a constant amplitude V_i and a uniformly distributed random phase $\theta_i \sim \mathcal{U}[0, 2\pi)$. The random phases for each dominant wave are assumed to be statistically independent.

Let $\gamma \triangleq \gamma_0 R^2$ be the instantaneous received SNR through, where $\gamma_0 \triangleq P_T/N_0$ is defined as the transmit SNR, with P_T being the transmit power and N_0 being the mean power of the additive white Gaussian noise. Note that γ can also be redefined for the sake of convenience as $\gamma = \bar{\gamma}|h|^2$, where h denotes any normalized fading channel, i.e., $\mathbb{E}\{|h|^2\} = 1$ and $\bar{\gamma}$ representing the average receive SNR. According to the formulation in [13], the corresponding PDF and CDF of γ over NWDP fading channel are:

$$f_i(\gamma_i) = \frac{1}{\bar{\gamma}_i} \exp\left(-\frac{\gamma_i}{\bar{\gamma}_i}\right) \sum_{n_i=0}^{\infty} C_{n_i} L_{n_i}\left(\frac{\gamma_i}{\bar{\gamma}_i}\right), \quad (2a)$$

$$F_i(\gamma_i) = \sum_{n_i=0}^{\infty} C_{n_i} \sum_{k_i=0}^{n_i} \frac{(-1)^{k_i}}{k_i!} \binom{n_i}{k_i} \gamma \left(k_i + 1, \frac{\gamma_i}{\bar{\gamma}_i}\right), \quad (2b)$$

where $i \in \{B, E\}$ represents either the main channel or the eavesdropper channel, $\bar{\gamma}_i$ is the average receive SNR at B or E as previously stated, i.e.,

$$\bar{\gamma}_i = \gamma_0 \mathbb{E}[R_i^2] r_i^{-\eta_i} = \gamma_0 \left(\sum_{n=0}^{N_i} V_{n,i}^2 + \Omega_i \right) r_i^{-\eta_i}, \quad (3)$$

where η_i is the path-loss exponent, and r_i is the propagation distance². The C_{n_i} coefficient can be calculated recursively by [13]

$$C_{n_i} = \sum_{k_i=0}^{n_i} \frac{(-\epsilon_i)^{k_i}}{k_i!} \binom{n_i}{k_i} u_{N_i+1}^{(2k_i)}, \quad (4)$$

¹We note that the consideration of arbitrary N in (1) allows for individually accounting for the effect of having multiple specular waves and largely differs from the conventional assumptions in fading modeling, reducing only for $N = 0, 1, 2$ to the Rayleigh, Rician and TWDP cases, respectively [4].

²Here, as in the LOS ball blockage model, we assume that r_i lies within a sphere of fixed radius R_B . Interested readers can revise [18] for further guidance about simplification of the LOS region as a fixed equivalent LOS ball in mm-Wave cellular networks.

where $\epsilon_i = (\mathbb{E} [R_i^2])^{-1}$, and

$$u_j^{2k_i} = \sum_{m=0}^{k_i} \binom{k_i}{m}^2 u_{j-1}^{(2m)} v_j^{(2k_i-2m)}, \text{ for } j = 2, \dots, N_i + 1, \quad (5)$$

where the initial value is $u_1^{2k_i} = v_1^{2k_i}$, and

$$v_j^{2k_i} = \begin{cases} V_{j,i}^{2k_i}, & \text{for } j = 1 \dots N_i, \\ (1)_{k_i} (\Omega_i)^{k_i}, & \text{for } j = N_i + 1. \end{cases} \quad (6)$$

III. SECRECY OUTAGE PROBABILITY ANALYSIS

A. Exact SOP Analysis

We consider a passive eavesdropping scenario, so that Alice has no channel state information (CSI) of Eve's channel. Hence, Alice's only choice is to encode the confidential data into codewords at a constant rate R_S . This can occur in a practical setup where Eve is silent during all transmissions. According to [19], the secrecy capacity is obtained as

$$\begin{aligned} C_S &= \max \{C_B - C_E, 0\} \\ &= \max \{\log_2(1 + \gamma_B) - \log_2(1 + \gamma_E), 0\} \end{aligned} \quad (7)$$

With these considerations, secrecy is achieved only in those instants on which $R_S \leq C_S$, and is compromised otherwise. In this context, the SOP is defined as the probability that the instantaneous secrecy capacity C_S falls below a target secrecy rate threshold R_S , and can be expressed as [7]

$$\begin{aligned} \text{SOP} &= \Pr \{C_S(\gamma_B, \gamma_E) < R_S\} \\ &= \Pr \left\{ \left(\frac{1 + \gamma_B}{1 + \gamma_E} \right) < 2^{R_S} \triangleq \tau \right\} \\ &= \Pr \{ \gamma_B < \tau \gamma_E + \tau - 1 \} \\ &= \int_0^\infty F_{\gamma_B}(\tau \gamma_E + \tau - 1) f_{\gamma_E}(\gamma_E) d\gamma_E. \end{aligned} \quad (8)$$

Furthermore, a high SNR approximation of the SOP can be obtained from (8) as

$$\text{SOP}_A = \Pr \{ \gamma_B < \tau \gamma_E \} \leq \text{SOP}. \quad (9)$$

Substituting (2) into (8) and (9), we can obtain the SOP and the SOP_A , respectively, over NWDP fading channels in the following Lemma.

Lemma 1. *The SOP and the SOP_A over NWDP fading channels can be obtained as (10) and (11), respectively, at the top of the next page.*

Proof. See Appendix A. \square

Remark 1. Notice that the derived analytical expressions for both the SOP and SOP_A are expressed in terms of infinite series representations. This is also the case of the analysis in [11] for TWDP based on the *approximate* PDF in [4], which arises as a special case of our analysis.

B. Asymptotic Analysis

To get further insights about the role of the fading parameters in the system performance, the main concern in this section is to derive asymptotic closed-form expressions to investigate the behavior of the SOP given in (8) at high-SNR regime. Here, we assume the following scenarios: (i) both $\bar{\gamma}_B$ and $\bar{\gamma}_E$ go to infinity, while the ratio between these SNRs is kept unchanged³; (ii) $\bar{\gamma}_B \rightarrow \infty$ while $\bar{\gamma}_E$ is kept fixed⁴. Our goal would be obtaining asymptotic expressions in the form $\text{SOP}^\infty \approx G_c \bar{\gamma}_B^{-G_d}$, where G_c and G_d represent the secrecy array gain and the secrecy diversity gain, respectively. However, as we will later see, such expressions will not be of much practical use as in many cases, such asymptotic does not kick in until very low probabilities are considered. Hence, our asymptotic expressions will incorporate additional terms on which the exponent of $\bar{\gamma}_B$ play a relevant role on the SOP decay for practical operational values. Next, the corresponding asymptotic expressions of the SOP over NWDP fading channels are given in the following Lemma.

Lemma 2. *The asymptotic closed-form expressions of the SOP over NWDP fading channels for the cases in that both $\bar{\gamma}_B \rightarrow \infty, \bar{\gamma}_E \rightarrow \infty$, and only $\bar{\gamma}_B \rightarrow \infty$ can be obtained as (12) and (13), respectively, at the top of the next page.*

Proof. See Appendix B. \square

IV. NUMERICAL RESULTS AND DISCUSSIONS

In this section, we validate the accuracy of the proposed expressions⁵ for some representative cases via Monte Carlo simulations. We define a power ratio parameter similar to the well-known Rician K parameter, e.g., $K_{N_i} \triangleq \frac{\Omega_{N_i}}{\Omega_i}$, with $\Omega_{N_i} = \sum_{n=0}^{N_i} V_{n,i}^2$ being the total average power of the specular components. For the sake of comparison, the Rayleigh case (i.e., $N_B = N_E = 0$) is included as a reference.

Before getting into the numerical examples, an important remark is in order. Herein, we emphasize on providing clear evidence to identify the impact of increasing/decreasing both the number and the power of the dominant specular waves over the secrecy performance. In other words, we aim to determine to what extent it is worth that each of the individual specular waves is treated separately, or it can be safely incorporated into the diffuse component.

In Fig. 2, we compare the SOP as a function of $\bar{\gamma}_B$ for different values of dominant specular components $N_B =$

³This scenario corresponds to the case when both B and E are close to A.

⁴This scenario corresponds to the case that A is very close to B and E is located far way.

⁵Here, it is worth mentioning that depending on the value of the involved channel parameters, these series require different number of terms to attain an accurate approximation. In this context, the overall convergence speed of these series is achieved faster for small values of both dominant rays (e.g., N_B , and N_E) and power of Bob's dominant specular components (i.e., K_{dB}^B). For instance, exhaustive tests have shown that the number of terms to arrive at the desired accuracy (e.g., 10^{-6}) varied from 20 to 30 at Bob and from 4 to 10 at Eve, and the average elapsed times to obtain the aforementioned accuracy were $\sim 14.1, 27.5, 81.7, 103.5, 114.6$ seconds for $N = 1, \dots, 5$, respectively. Moreover, the mathematical representation of the derived series consists of well-known elementary and special functions, which can be easily implemented in software for numerical evaluation.

$$\begin{aligned} \text{SOP} &= 1 - \sum_{n_B=0}^{\infty} C_{n_B} \sum_{k_B=0}^{n_B} (-1)^{k_B} \binom{n_B}{k_B} \left(\frac{1}{\bar{\gamma}_E}\right) \sum_{n_E=0}^{\infty} C_{n_E} \sum_{q=0}^{k_B} \frac{1}{q!} \left(\frac{1}{\bar{\gamma}_B}\right)^q \exp\left(-\frac{\tau-1}{\bar{\gamma}_B}\right) \sum_{a=0}^q \binom{q}{a} (\tau-1)^{q-a} \tau^a \\ &\quad \times \left(\frac{1}{\bar{\gamma}_E} + \frac{\tau}{\bar{\gamma}_B}\right)^{-1-a} \Gamma(1+a) {}_2F_1\left(1+a, -n_E; 1; \frac{\bar{\gamma}_B}{\bar{\gamma}_B + \bar{\gamma}_E \tau}\right) \end{aligned} \quad (10)$$

$$\begin{aligned} \text{SOP}_A &= 1 - \sum_{n_B=0}^{\infty} C_{n_B} \sum_{k_B=0}^{n_B} (-1)^{k_B} \binom{n_B}{k_B} \left(\frac{1}{\bar{\gamma}_E}\right) \sum_{n_E=0}^{\infty} C_{n_E} \sum_{q=0}^{k_B} \frac{1}{q!} \left(\frac{\tau}{\bar{\gamma}_B}\right)^q \left(\frac{1}{\bar{\gamma}_E} + \frac{\tau}{\bar{\gamma}_B}\right)^{-1-q} \Gamma(1+q) \\ &\quad \times {}_2F_1\left(-n_E, 1+q; 1; \frac{\bar{\gamma}_B}{\bar{\gamma}_B + \bar{\gamma}_E \tau}\right) \end{aligned} \quad (11)$$

$$\text{SOP}^{\infty} \approx \sum_{n_B=0}^{\infty} C_{n_B} \sum_{k_B=0}^{n_B} \frac{(-1)^{k_B}}{(k_B+1)!} \binom{n_B}{k_B} \left(\frac{\tau}{\bar{\gamma}_B}\right)^{k_B+1} \sum_{n_E=0}^{\infty} C_{n_E} \sum_{k_E=0}^{n_E} \frac{(-1)^{k_E}}{k_E!} \binom{n_E}{k_E} \left(\frac{1}{\bar{\gamma}_E}\right)^{k_E+1} \sum_{i=1}^n w_i \exp(l_i) l_i^{k_B+k_E+1} \quad (12)$$

$$\text{SOP}^{\infty} \approx \sum_{n_B=0}^{\infty} C_{n_B} \sum_{k_B=0}^{n_B} \frac{(-1)^{k_B}}{(k_B+1)!} \binom{n_B}{k_B} \left(\frac{\tau \bar{\gamma}_E}{\bar{\gamma}_B}\right)^{k_B+1} \sum_{n_E=0}^{\infty} C_{n_E} \frac{\Gamma(k_B+2) \Gamma(n_E+1)}{n_E!} {}_2F_1(-n_E, k_B+2; 1; \bar{\gamma}_E) \quad (13)$$

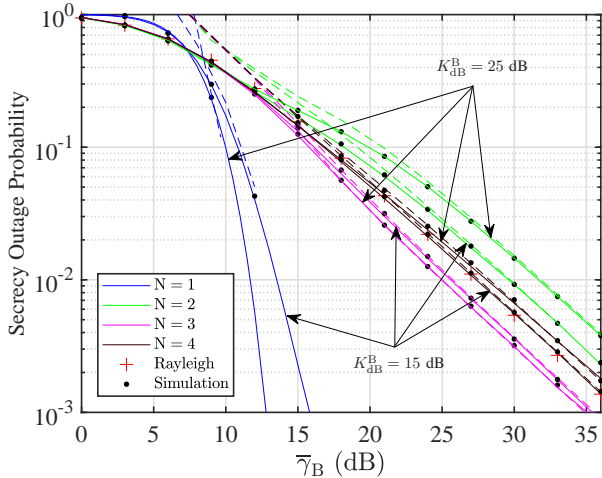


Fig. 2. SOP vs. $\bar{\gamma}_B$, for different numbers of dominant specular waves N by considering balanced amplitude scenario (i.e., $V_{n,i} = 1$ for $n = 1, \dots, N_i$). For all curves, the parameter values are: $R_S = 1$ bps/Hz, $\bar{\gamma}_E = 4$ dB, $K_{dB}^E = 10$ dB, $\Omega_i = 1$, and $N_i = N$ for $i \in \{B, E\}$. Dashed lines correspond to asymptotic analysis by using expression (12).

$N_E = N$, by considering the case of balanced amplitudes, i.e., $V_{n,B} = V_{n,E} \forall B, n = 1 \dots N$. For this scenario, the corresponding fading parameters are given by: $K_{dB}^B = 10 \log_{10}(K_B = K_{N_B}) \in \{8, 25\}$ dBs with $K_{dB}^E = 0$ dB, $R_S = 1$ bps/Hz, and $\bar{\gamma}_E = 1$ dB. Note that in all instances, Monte Carlo simulations perfectly match with our derived results.

We see that the secrecy performance does not monotonically increase with the number of specular components; instead, we see that the cases with $N_B = 1$ and $N_B = 2$ bound the secrecy

performance when the rest of parameters are fixed. This is in coherence with the fact that for an even number of dominant specular components of equal amplitudes, the probability of total cancellation between them is larger than when an odd number is considered [17]. This increases fading severity for the desired link more relevantly for large K , which ultimately degrades the SOP. We also see that for $N = 4$, the performance is very similar than in the Rayleigh case (i.e., $N \rightarrow \infty$).

In Fig. 3, we now evaluate the SOP vs. $\bar{\gamma}_B$ for different numbers of dominant specular components $N_B = N_E = N$ by considering an unbalanced amplitudes scenario. For simplicity, yet without loss of generality, the amplitudes of successive rays are expressed in terms of the amplitude of the first dominant component, as proposed in [12], that is, $V_{n,i} = \alpha_{n,i} V_{1,i}$ for $n = 2, \dots, N_i$, with $0 < \alpha_{n,i} < 1$ and $i \in \{B, E\}$. Considering this, we set: $\alpha_{n,i} = \alpha_B = \alpha_E = 0.3$ with $K_{dB}^B \in \{8, 25\}$ dBs, $K_{dB}^E = 0$ dB, $R_S = 1$ bps/Hz, and $\bar{\gamma}_E = 1$ dB. Here, we investigate the impact of increasing both the number and the power of Bob's dominant rays for the case of unbalanced amplitudes. We observe in all traces that, unlike on the balanced counterpart, the SOP performance now monotonically improves when rising K_{dB}^B or lowering N , regardless of whether it is even or odd. It can be observed that a reduced number of dominant specular components at Bob is now beneficial from a secrecy perspective. We also see that in all cases, the SOP performance is always better than its Rayleigh counterpart. Regarding the asymptotic behaviour, it can be noticed that the asymptotic plots accurately approximate the SOP curves at high SNR regime. Additionally, all curves have different slopes. The reason for this will be discussed later.

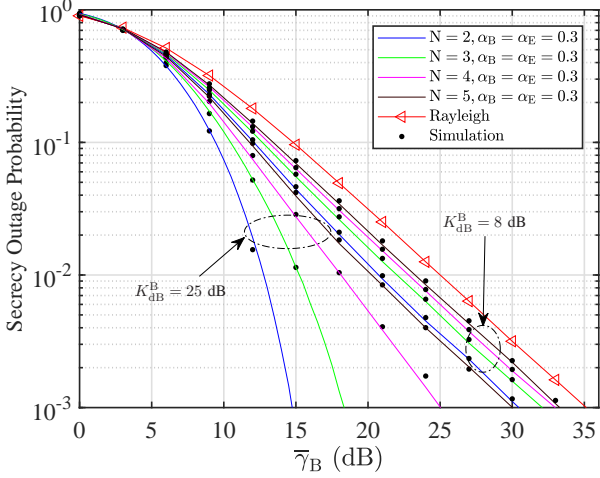


Fig. 3. SOP in terms of $\bar{\gamma}_B$ for different numbers of dominant specular waves N , by considering unbalanced amplitude case (i.e., $\alpha_{n,i} = \alpha_i = 0.3$). For all cases, the corresponding parameters are set to the following values: $R_S = 1$ bps/Hz, $\bar{\gamma}_E = 1$ dB, $K_{dB}^B = 0$ dB, $\Omega_i = 1$, and $N_i = N$ for $i \in \{B, E\}$.

In Fig. 4, we evaluate both the SOP and the SOP_A as a function of $\bar{\gamma}_B$, in order to understand the interplay between the number of dominant specular components $N_B = N_E = N$, the amplitude imbalance and the power of the dominant components. We use a similar set of parameters as those in Fig. 3, except for $\{\alpha_B, \alpha_E\} = \{0.2, 0.9\}$, $\{\alpha_B, \alpha_E\} = \{0.9, 0.2\}$, and $\bar{\gamma}_E = 8$ dB. We now observe that the worst secrecy performance is attained for cases where the imbalance for the legitimate user α_B is smaller than that of α_E , i.e. when $\alpha_B > \alpha_E$. Therefore, for the cases where α_B is lower than α_E , we can obtain the desired secrecy performance (i.e., a target SOP) for a lower average SNR at Bob. In such case, some other interesting observations can be made: (i) the SOP performance under NWDOP fading is much better than in the Rayleigh case, and (ii) the increase on the number of dominant specular rays arriving at Bob is detrimental from a secrecy perspective.

On the other hand, the worst SOP performances are achieved for the case with $(\alpha_B = 0.9, \alpha_E = 0.2)$, which is explained as follows: because the amplitudes for the legitimate link are balanced, this is translated into a more severe fading; conversely, the unbalanced amplitudes for the eavesdropper's link indicate a lower fading severity compared to the Rayleigh case. Combining the two effects, the overall SOP performance is hence worse than when assuming Rayleigh fading for both links.

Fig. 5 presents the evolution of the SOP as a function of R_S , considering the following channel settings: $\bar{\gamma}_E = 1$ dB, $\bar{\gamma}_B = 8$ dB, $K_{dB}^B = K_{dB}^E = 20$ dB, and $\{\alpha_B, \alpha_E\} = \{0.2, 0.3\}$. Herein, we analyze the effect of having a different number of dominant specular rays at both Bob and Eve over the secrecy performance. We consider the cases $N_E = \{2, 3\}$ and $N_B = \{2, 3, 4, 5\}$, and for the sake of comparison, we also include the case $N_B = N_E$. Once again we see that having a larger number of multipath waves at the legitimate receiver in this unbalanced scenario effectively increases channel variability,

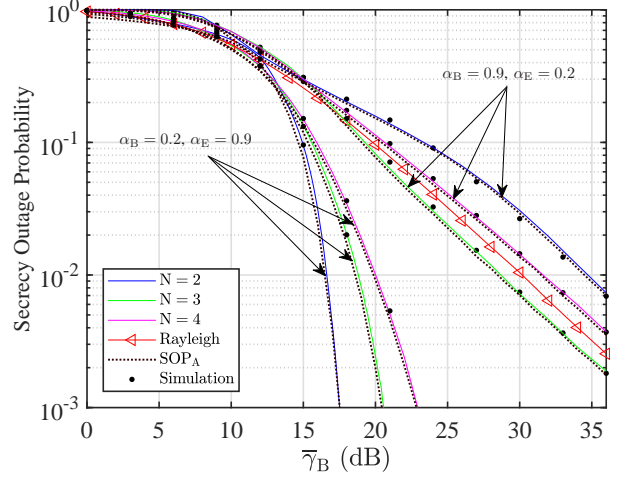


Fig. 4. SOP vs. $\bar{\gamma}_B$ for different numbers of dominant specular waves N by considering unbalanced amplitude case (i.e., $\{\alpha_B, \alpha_E\} = \{0.2, 0.9\}$ and $\{\alpha_B, \alpha_E\} = \{0.9, 0.2\}$). For all curves, the values of channel parameters are: $R_S = 1$ bps/Hz, $\bar{\gamma}_E = 8$ dB, $K_{dB}^B = K_{dB}^E = 25$ dB, $\Omega_i = 1$, and $N_i = N$ for $i \in \{B, E\}$.

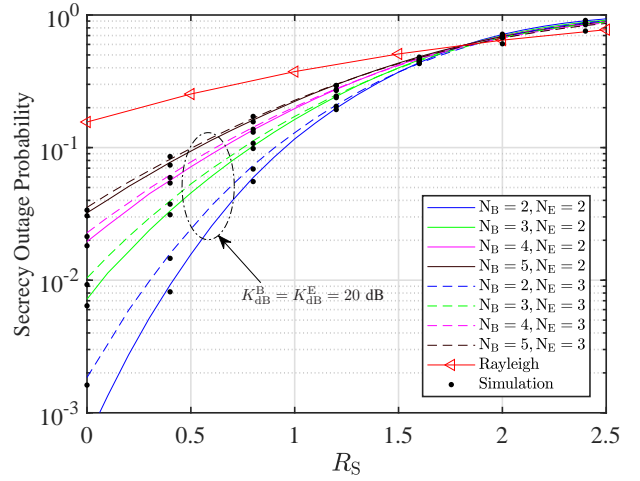


Fig. 5. SOP in terms of R_S for different numbers of dominant specular waves of $N_B = \{2, 3, 4, 5\}$ with regard to $N_E = \{2, 3\}$ by considering unbalanced amplitude case (i.e., $\{\alpha_B, \alpha_E\} = \{0.2, 0.3\}$). For all curves, we set: $\bar{\gamma}_E = 1$ dB, $\bar{\gamma}_B = 8$ dB, $K_{dB}^B = K_{dB}^E = 20$ dB, and $\Omega_i = 1$ for $i \in \{B, E\}$.

which causes the SOP obtained when transmitting at a rate R_S to be increased with N_B . We also see that for a fixed N_B , increasing the number of rays on the eavesdropper's channel is also detrimental for the SOP. This can be understood by recalling that in the presence of a single dominant specular component for each link and a strong LOS condition, the setup almost reduces to the AWGN case, for which the SOP is zero as $\bar{\gamma}_B > \bar{\gamma}_E$. Hence, having a reduced number of rays and a dominant component much larger than the remaining specular waves turn out being beneficial for physical layer security.

Next, Fig. 6 illustrates the SOP vs. $\bar{\gamma}_B$ for different numbers of rays $N_B = N_E = N$ with $\bar{\gamma}_E = 1$ dB, $K_{dB}^B = 25$ dB, and $K_{dB}^E = 0$ dB. Moreover, we set: $R_S = \{1, 2.5\}$ with $\alpha =$

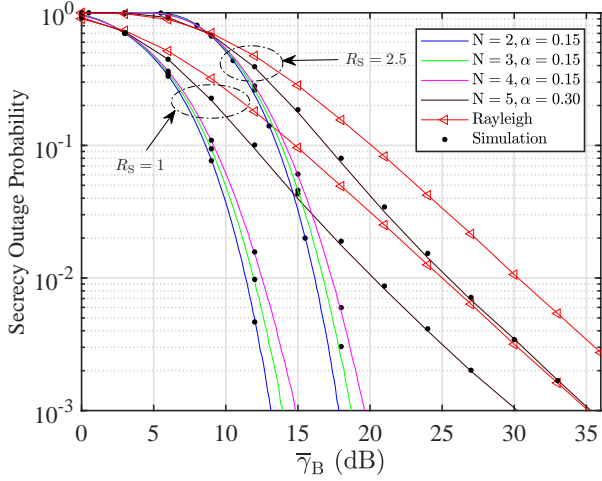


Fig. 6. SOP vs. $\bar{\gamma}_B$ for different numbers of dominant specular waves $N = N_B = N_E$ by varying the value of R_S and assuming unbalanced amplitudes (i.e., $\alpha = \{0.15, 0.30\}$). Also, $\bar{\gamma}_E = 1$ dB, $K_{dB}^B = 25$ dB, and $K_{dB}^E = 0$ dB.

$\alpha_B, = \alpha_E = 0.15$ and $\alpha = \alpha_B, = \alpha_E = 0.30$ for $N = 2, \dots, 4$, and $N = 5$, respectively. From the figure can be observed that both the relative amplitudes and the number of the dominant waves play a pivotal role on the secrecy performance. For instance, we see that the decay of the SOP is rather abrupt for $\alpha = 0.15$ and $N = 1, \dots, 4$ regardless of the choice of $R_S = \{1, 2.5\}$. However, when both the number of rays and the relative amplitudes of the rays are slightly increased (say $\alpha = 0.3$ and $N = 5$), then the SOP is dramatically impaired and the decay is now similar to the Rayleigh case. This is in coherence with the observations made in [12] in the limit case of the absence of diffuse scattering, as $\alpha(N_B - 1) < 1$.

Finally, in Fig. 7, we plot the SOP vs. $\bar{\gamma}_B$ and the two asymptotic results (12), (13), respectively. In all the cases, we employ equal numbers of rays at both B and E, i.e., $N = N_B = N_E$, $R_S = 1$ bps/Hz, $\Omega_B = \Omega_E = 1$, and $\bar{\gamma}_E = 8$ dB. Also, yet without loss of generality, we assume the following cases: *Case I* ($N = 1$): Balanced amplitudes, $V_{1,B} = V_{1,E} = 1$, and $K_{dB}^B = K_{dB}^E = 10$ dB; *Case II* ($N = 2$): Unbalanced amplitudes, $V_{2,i} = \alpha_{2,i}V_{1,i}$ with $V_{1,i} = 1$ for $i \in \{B, E\}$, $\alpha_{2,B} = 0.2$, $\alpha_{2,E} = 0.9$, and $K_{dB}^B = K_{dB}^E = 15$ dB; *Case III* ($N = 3$): Unbalanced amplitudes, $V_{n,i} = \alpha_{n,i}V_{1,i}$ with $V_{1,i} = 1$ for $i \in \{B, E\}$, $\alpha_{n,i} = \alpha_B = \alpha_E = 0.3$ for $n = 2, 3$, and $K_{dB}^B = K_{dB}^E = 10$ dB. Here, our primary aim is to analyze the secrecy diversity order of the main links in the proposed scenarios. Firstly, based on the asymptotic expressions (i.e., (12), and (13)), we see that the exponents for the $\bar{\gamma}_B$ terms depend on one of the summation indexes (i.e., $(k_B + 1)$). This suggests that each of these terms contributes in different ways to the decay of the SOP, which explains that the slope of the SOP is different depending on the range of values of $\bar{\gamma}_B$. As the SNR is increased, it is only the first term of the series which contributes to the SOP, revealing a diversity order of one (vide all cases in Fig. 7). However, we can see that such diversity order is not useful for *Case II*, which justifies the need

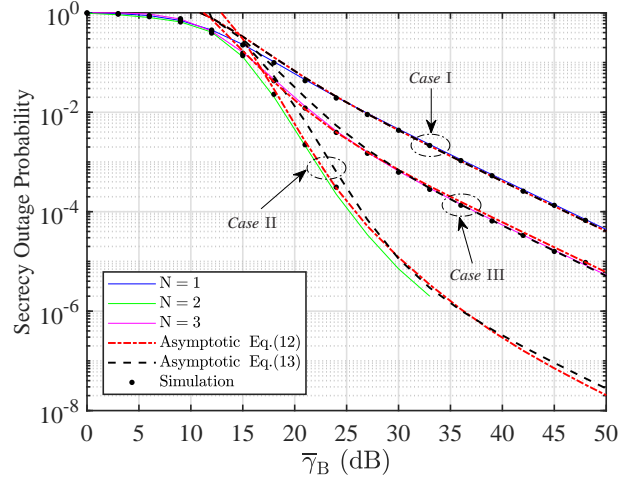


Fig. 7. SOP vs. $\bar{\gamma}_B$ for different numbers of dominant specular waves $N = N_B = N_E$ by assuming for all cases $R_S = 1$ bps/Hz, $\Omega_B = \Omega_E = 1$, and $\bar{\gamma}_E = 8$ dB.

of the more accurate asymptotic expressions here provided, compared to those only relying on G_d expression. Also, we can observe that the asymptotic analytical in (12) is tighter than the asymptotic one given in (13).

V. CONCLUSIONS

We investigated how the explicit consideration of the incident waves arriving at the receiver ends may impact physical layer security performance in the context of wireless fading channels. The analytical results here presented complement and generalize those previously reported in the literature, and support the need of using ray-based fading models in those situations on which a reduced number of multipath waves are considered. The main takeaways of our work can be summarized as: (i) abundant dominant specular rays impair the SOP, so scenarios with a reduced number of rays arriving at both Bob and Eve are beneficial whenever $\bar{\gamma}_B > \bar{\gamma}_E$; (ii) balanced amplitudes for the eavesdropper's link and unbalanced amplitudes for the desired link are the most favorable case from a PLS perspective; (iii) a significant increase on the power of Bob's dominant specular components with respect to the power of Eve's dominant specular components (i.e., $K_B \gg K_E$), in the case of balanced amplitudes, is a worst case scenario for secrecy performance.

APPENDIX A
PROOFS OF LEMMA 1

A. SOP

Substituting (2) into (8), we can obtain

$$\begin{aligned} \text{SOP} &= \underbrace{\sum_{n_B=0}^{\infty} C_{n_B} \sum_{k_B=0}^{n_B} \frac{(-1)^{k_B}}{k_B!} \binom{n_B}{k_B} \frac{1}{\bar{\gamma}_E} \sum_{n_E=0}^{\infty} C_{n_E}}_{C_1} \\ &\quad \times \underbrace{\int_0^{\infty} \exp\left(-\frac{\gamma_E}{\bar{\gamma}_E}\right) L_{n_E}\left(\frac{\gamma_E}{\bar{\gamma}_E}\right)}_{I_1} \\ &\quad \times \underbrace{\gamma \left(k_B + 1, \frac{(\tau\gamma_E + \tau - 1)}{\bar{\gamma}_B}\right)}_{I_1} d\gamma_E. \end{aligned} \quad (14)$$

Using [20, Eq. (8.352.1)] into (14), I_1 can be rewritten as

$$\begin{aligned} I_1 &= k_B! \underbrace{\int_0^{\infty} \exp\left(-\frac{\gamma_E}{\bar{\gamma}_E}\right) L_{n_E}\left(\frac{\gamma_E}{\bar{\gamma}_E}\right) d\gamma_E}_{I_2} \\ &\quad - k_B! \sum_{q=0}^{k_B} \frac{1}{q!} \left(\frac{1}{\bar{\gamma}_B}\right)^q \underbrace{\int_0^{\infty} \exp\left(-\frac{\gamma_E}{\bar{\gamma}_E}\right)}_{I_3} \\ &\quad \times \underbrace{L_{n_E}\left(\frac{\gamma_E}{\bar{\gamma}_E}\right) \exp\left(-\frac{\tau\gamma_E + \tau - 1}{\bar{\gamma}_B}\right)}_{I_3} \\ &\quad \times \underbrace{(\tau\gamma_E + \tau - 1)^q}_{I_3} d\gamma_E. \end{aligned} \quad (15)$$

Here, with the help of [20, Eq. (7.414.6)] the value of the integral I_2 can be $\bar{\gamma}_E$ when $n_E = 0$ or zero otherwise (i.e., $n_E \neq 0$). In the former case, after by performing some algebraic manipulations, the first term of the SOP can be simplified as $C_1 k_B! \bar{\gamma}_E = 1$. Next, by using [20, Eq. (1.111)], I_3 can be expressed as

$$\begin{aligned} I_3 &= \sum_{a=0}^q \binom{q}{a} (\tau - 1)^{q-a} \tau^a \exp\left(-\frac{\tau - 1}{\bar{\gamma}_B}\right) \underbrace{\int_0^{\infty} L_{n_E}\left(\frac{\gamma_E}{\bar{\gamma}_E}\right)}_{I_4} \\ &\quad \times \underbrace{\gamma_E^a \exp\left(-\frac{\gamma_E}{\bar{\gamma}_E} - \frac{\tau\gamma_E}{\bar{\gamma}_B}\right) d\gamma_E}_{I_4}. \end{aligned} \quad (16)$$

Then, by solving the corresponding integral in I_4 , we get

$$\begin{aligned} I_4 &= \left(\frac{1}{\bar{\gamma}_E} + \frac{\tau}{\bar{\gamma}_B}\right)^{-1-a} \Gamma(1+a) \\ &\quad \times {}_2F_1\left(1+a, -n_E, 1, \frac{\bar{\gamma}_B}{\bar{\gamma}_B + \bar{\gamma}_E \tau}\right). \end{aligned} \quad (17)$$

Next, by combining (14) to (17), the SOP can be formulated as in (10), which concludes the proof.

B. SOP_A

Substituting (2) into (9), we get

$$\begin{aligned} \text{SOP}_A &= \underbrace{\sum_{n_B=0}^{\infty} C_{n_B} \sum_{k_B=0}^{n_B} \frac{(-1)^{k_B}}{k_B!} \binom{n_B}{k_B} \frac{1}{\bar{\gamma}_E} \sum_{n_E=0}^{\infty} C_{n_E}}_{C_1} \\ &\quad \times \underbrace{\int_0^{\infty} \exp\left(-\frac{\gamma_E}{\bar{\gamma}_E}\right) L_{n_E}\left(\frac{\gamma_E}{\bar{\gamma}_E}\right)}_{I_5} \\ &\quad \times \underbrace{\gamma \left(k_B + 1, \frac{\tau\gamma_E}{\bar{\gamma}_B}\right)}_{I_5} d\gamma_E. \end{aligned} \quad (18)$$

Again, by using [20, Eq. (8.352.1)] into (18), I_5 can be reformulated as

$$\begin{aligned} I_5 &= k_B! \underbrace{\int_0^{\infty} \exp\left(-\frac{\gamma_E}{\bar{\gamma}_E}\right) L_{n_E}\left(\frac{\gamma_E}{\bar{\gamma}_E}\right) d\gamma_E}_{I_5} \\ &\quad - k_B! \sum_{q=0}^{k_B} \frac{1}{q!} \left(\frac{1}{\bar{\gamma}_B}\right)^q \tau^q \underbrace{\int_0^{\infty} \exp\left(-\frac{\gamma_E}{\bar{\gamma}_E}\right)}_{I_6} \\ &\quad \times \underbrace{L_{n_E}\left(\frac{\gamma_E}{\bar{\gamma}_E}\right) \exp\left(-\frac{\tau\gamma_E}{\bar{\gamma}_B}\right) \gamma_E^q}_{I_6} d\gamma_E. \end{aligned} \quad (19)$$

Here, note that I_5 is equivalent to I_2 . Therefore, the first term of the SOP_A (i.e., $C_1 k_B! \bar{\gamma}_E$) once again equals unity, as discussed in the previous proof. On the other hand, by solving the corresponding integral in I_6 , yields

$$\begin{aligned} I_6 &= \left(\frac{1}{\bar{\gamma}_E} + \frac{\tau}{\bar{\gamma}_B}\right)^{-1-q} \Gamma(1+q) \\ &\quad \times {}_2F_1\left(-n_E, 1+q, 1, \frac{\bar{\gamma}_B}{\bar{\gamma}_B + \bar{\gamma}_E \tau}\right). \end{aligned} \quad (20)$$

Finally, by combining (18) to (20), the SOP_A is reached as in (11), which completes the proof.

APPENDIX B
PROOFS OF LEMMA 2

A. SOP[∞]

1) *Keeping $\bar{\gamma}_E$ Fixed and $\bar{\gamma}_B \rightarrow \infty$* : In order to approximate (2b) as $\bar{\gamma}_B \rightarrow \infty$, we use the following relationship $\gamma(a, x) \approx x^a/s$ as $x \rightarrow 0$. Therefore, (2b) can be asymptotically expressed by

$$F_B(\gamma_B) \approx \sum_{n_B=0}^{\infty} C_{n_B} \sum_{k_B=0}^{n_B} \frac{(-1)^{k_B}}{(k_B + 1)!} \binom{n_B}{k_B} \left(\frac{\gamma_B}{\bar{\gamma}_B}\right)^{k_B+1}. \quad (21)$$

Substituting (21) together with (2a) into (9), it follows that

$$\begin{aligned} \text{SOP}^{\infty} &\approx \sum_{n_B=0}^{\infty} C_{n_B} \sum_{k_B=0}^{n_B} \frac{(-1)^{k_B}}{(k_B + 1)!} \binom{n_B}{k_B} \left(\frac{1}{\bar{\gamma}_E}\right) \left(\frac{\tau}{\bar{\gamma}_B}\right)^{k_B+1} \\ &\quad \times \sum_{n_E=0}^{\infty} C_{n_E} \underbrace{\int_0^{\infty} \gamma_E^{k_B+1} \exp\left(-\frac{\gamma_E}{\bar{\gamma}_E}\right) L_{n_E}\left(\frac{\gamma_E}{\bar{\gamma}_E}\right) d\gamma_E}_{I_7} \end{aligned} \quad (22)$$

Next, with the aid of [20, Eq. (7.414.7)] to solve the integral in I_7 , the asymptotic SOP can be expressed as in (13), which concludes the proof.

2) Both $\bar{\gamma}_E \rightarrow \infty$, $\bar{\gamma}_B \rightarrow \infty$, and Fixed Ratio $\bar{\gamma}_E/\bar{\gamma}_B$: From (21), the asymptotic PDF of E (i.e., $\bar{\gamma}_E \rightarrow \infty$) is given by

$$f_E(\gamma_E) \approx \sum_{n_E=0}^{\infty} C_{n_E} \sum_{k_E=0}^{n_E} \frac{(-1)^{k_E}}{k_E!} \binom{n_E}{k_E} \left(\frac{1}{\bar{\gamma}_E}\right)^{k_E+1} \gamma_E^{k_E}. \quad (23)$$

Substituting (21) and (23) into (9), we have

$$\begin{aligned} \text{SOP}^\infty &\approx \sum_{n_B=0}^{\infty} C_{n_B} \sum_{k_B=0}^{n_B} \frac{(-1)^{k_B}}{(k_B+1)!} \binom{n_B}{k_B} \left(\frac{\tau}{\bar{\gamma}_B}\right)^{k_B+1} \\ &\times \sum_{n_E=0}^{\infty} C_{n_E} \sum_{k_E=0}^{n_E} \frac{(-1)^{k_E}}{k_E!} \binom{n_E}{k_E} \left(\frac{1}{\bar{\gamma}_E}\right)^{k_E+1} \\ &\times \underbrace{\int_0^\infty \gamma_E^{k_B+k_E+1} d\gamma_E}_{I_8}. \end{aligned} \quad (24)$$

To solve I_8 , one can rewrite it as

$$I_8 = \int_0^\infty \exp(-\gamma_E) f(\gamma_E) d\gamma_E, \quad (25)$$

where $f(\gamma_E) = \exp(\gamma_E) \gamma_E^{k_B+k_E+1}$. Now, according to the Gauss-Laguerre quadrature method [15, Eq. (25.4.45)], I_8 can be closely approximated by a weighted sum as

$$I_8 \approx \sum_{i=1}^n w_i f(l_i), \quad (26)$$

in which l_i is the i th zero of the Laguerre polynomial $L_n(\gamma_E)$ [15, Eq. (22.2.13)], and $w_i = l_i [(n+1)L_{n+1}(l_i)]^{-2}$.⁶This completes the proof.

REFERENCES

- [1] D. Liu, W. Hong, T. S. Rappaport, C. Luxey and W. Hong, "What will 5G Antennas and Propagation Be?," *IEEE Trans. Antennas Propag.*, vol. 65, no. 12, pp. 6205–6212, Dec. 2017.
- [2] M. K. Samimi, G. R. MacCartney, S. Sun, and T. S. Rappaport, "28 GHz Millimeter-Wave Ultrawideband Small-Scale Fading Models in Wireless Channels," in *2016 IEEE 83rd Veh. Technol. Conf. (VTC-Spring)*, May 2016.
- [3] G. Taricco, "On the Convergence of Multipath Fading Channel Gains to the Rayleigh Distribution," *IEEE Wireless Commun. Lett.* vol. 4, no. 5, pp. 549–552, Oct. 2015.
- [4] G. D. Durgin, T. S. Rappaport, and D. A. de Wolf, "New Analytical Models and Probability Density Functions for Fading in Wireless Communications," *IEEE Trans. Commun.*, vol. 50, no. 6, pp. 1005–1015, Jun. 2002.
- [5] J. M. Romero-Jerez, F. J. López-Martínez, J. F. Paris, and A. J. Goldsmith, "The Fluctuating Two-Ray Fading Model: Statistical Characterization and Performance Analysis," *IEEE Trans. Wireless Commun.*, vol. 16, no. 7, pp. 4420–4432, Jul. 2017.
- [6] J. M. Romero-Jerez, F. J. López-Martínez, J. F. Paris, and A. Goldsmith, "The Fluctuating Two-Ray Fading Model for mmWave Communications," in *Proc. IEEE Globecom Workshops (GC Wkshps)*, Washington, DC, USA, Dec. 2016, pp. 1–6.
- [7] M. Bloch, J. Barros, M. R. D. Rodrigues, and S. W. Mclaughlin, "Wireless Information-Theoretic Security," *IEEE Tran. Inf. Theory*, vol. 54, no. 6, pp. 2515–2534, Jun. 2008.
- [8] J. D. Vega Sánchez, L. Urquiza-Aguiar, and M. C. P. Paredes, "Physical Layer Security for 5G Wireless Networks: A Comprehensive Survey," in *2019 IEEE 3rd Cyber Security in Networking Conference (CSNet)*, to be published, 2019.
- [9] D. P. Moya Osorio, J. D. Vega Sánchez, and H. Alves, "Physical Layer Security for 5G and beyond," in *5G REF: The Essential 5G Reference Online*, John Wiley & Sons, 2019, ch. 1, pp. 1–19.
- [10] W. Zeng, J. Zhang, S. Chen, K. P. Peppas, and B. Ai, "Physical Layer Security Over Fluctuating Two-Ray Fading Channels," *IEEE Trans. Veh. Technol.*, vol. 67, no. 9, pp. 8949–8953, Sep. 2018.
- [11] L. Wang, N. Yang, M. ElKashlan, P. L. Yeoh, and J. Yuan, "Physical Layer Security of Maximal Ratio Combining in Two-Wave With Diffuse Power Fading Channels," *IEEE Trans. Inf. Forensics Security*, vol. 9, no. 2, pp. 247–258, Feb. 2014.
- [12] P. Ramírez-Espinosa, R. J. Sánchez-Alarcón, and F. J. López-Martínez "On the Beneficial Role of a Finite Number of Scatterers for Wireless Physical Layer Security," Oct. 2019, arXiv:1910.09856. [Online].
- [13] Y. J. Chun, "A Generalized Fading Model with Multiple Specular Components," Oct. 2018, arXiv:1810.05258. [Online].
- [14] J.M. Romero-Jerez, F.J. Lopez-Martinez, J.P. Pena-Martin, and A. Abdi, "Stochastic Fading Channel Models with Multiple Dominant Specular Components for 5G and Beyond," May 2019, arXiv:1905.03567 [Online].
- [15] Abramowitz, M. and Stegun, I. A., "Handbook of Mathematical Functions, *US Dept. Of Commerce, National Bureau Of Standards*, Washington DC, 1972.
- [16] G. D. Durgin, "Theory of Stochastic Local Area Channel Modeling for Wireless Communications," *PhD diss.*, Virginia Tech, 2000.
- [17] C. Chen and A. Abdi, "Bit error rate in multipath wireless channels with several specular paths," *Electronics Letters* vol. 47, no. 18, pp. 1046–1048, 1 September 2011.
- [18] T. Bai and R. W. Heath Jr., "Coverage and Rate Analysis for Millimeter-wave Cellular Networks," *IEEE Trans. Wireless Commun.*, vol. 14, no. 2, pp. 1100–1114, Feb. 2015.
- [19] A. D. Wyner, "The wiretap channel," *Bell Syst. Tech. J.*, vol. 54, no. 8, pp. 1355–1387, Oct. 1975.
- [20] I. S. Gradshteyn and I. M. Ryzhik, *Table of Integrals, Series and Products*, 7th ed., San Diego, CA, USA: Academic Press, 2007.

⁶Experience in tests carried out show that, for large values of n of the Laguerre polynomial, it becomes computationally hard to obtain a solution of the SOP^∞ . However, choosing $n = 2$ is a good rule of thumb that has proven to be highly accurate with little computational effort.